Diffusion Tensor MRI Phantom Exhibits Anomalous Diffusion

Allen Q. Ye*, Penny L. Hubbard Cristinacce, Feng-Lei Zhou, Ziying Yin, Geoff J.M. Parker, and Richard L. Magin

Abstract— **This paper reports diffusion weighted MRI measurements of cyclohexane in a novel diffusion tensor MRI phantom composed of hollow coaxial electrospun fibers (average diameter 10.2 μm). Recent studies of the phantom demonstrated its potential as a calibration standard at low b values (less than 1000 s/mm^2) for mean diffusivity and fractional anisotropy. In this paper, we extend the characterization of cyclohexane diffusion in this heterogeneous, anisotropic material to high b values (up to 5000 s/mm^2), where the apparent diffusive motion of the cyclohexane exhibits anomalous behavior (i.e., the molecular mean squared displacement increases with time raised to the fractional power 2α/β). Diffusion tensor MRI was performed at 9.4 T using an Agilent imaging scanner and the data fit to a fractional order Mittag-Leffler (generalized exponential) decay model. Diffusion along the fibers was found to be Gaussian (2α/β=1), while diffusion across the fibers was sub-diffusive (2α/β<1). Fiber tract reconstruction of the data was consistent with scanning electron micrograph images of the material. These studies suggest that this phantom material may be used to calibrate MR systems in both the normal (Gaussian) and anomalous diffusion regimes.**

I. Introduction

Researchers and clinicians interested in neural connectivity and brain microstructure use diffusion tensor magnetic resonance imaging (DTI) as a tool to characterize white matter fiber structure and integrity within the brain. DTI accomplishes this by its sensitivity to multi-scale diffusion processes affecting water in the brain. In a hindered environment (e.g. myelinated axons inhibiting diffusion), water will have a preferred direction of travel thus giving clues to fiber orientation. However, MRI is limited by a resolution that is one to two orders of magnitude greater than the dimensions of cells and individual axons, so finding the ground truth surrounding axonal structure – especially in human subjects – can be difficult [1]. In this paper, we look more closely at a physical phantom for DTI and observe that the diffusion of cyclohexane between the fibers falls in the anomalous regime.

For standard DTI, molecular self-diffusion of water is assumed to be the primary source of motion in free water in the brain. The molecular self-diffusion of water implies that the mean squared displacement varies linearly with elapsed time. This model assumes three primary conditions: 1. The behavior of all particles must be identical 2. The distribution of displacements must have a finite variance, and 3. The future displacement must be free of any influence from past [2]. This motion, when observed using DTI, leads to a mono-exponential decay of the MR signal. However, numerous papers have reported diffusion measurements in biological tissues that deviate from this standard Gaussian model – suggesting non-Gaussian properties (anomalous) behavior [3–5]. Previous literature [4,6] has showed that brain tissue is particularly anomalous and is a tissue of interest for anomalous diffusion measurements.

One anomalous model that has been proposed as a replacement for the mono-exponential model is the continuous time random walk (CTRW) model [6]. In this model, we generalize the statistics of the jump length, Δx, and the waiting time (in-between jumps), Δt to follow power laws that decay to fractional order. Hence, longer jumps and longer waiting times are less likely than short ones. By doing so, the mean squared displacement is now proportional to time raised to the fractional power of 2α/β. where α is the time-fractional exponent and β is the space-fractional exponent. The result can be expressed as:

$$\langle x^2(t)\rangle \sim t^{2\alpha/\beta} \qquad (1)$$

where $0 \le \alpha \le 1$ and $0 \le \beta \le 2$. When $2\alpha/\beta = 1$, the CTRW model simplifies to normal diffusion, if larger than 1, CTRW predicts super-diffusion, if less than 1, CTRW exhibits sub-diffusion, as seen in Fig. 1. The CTRW model is attractive because it requires no *a priori* knowledge about the governing statistics surrounding the diffusion process.

Recently, a new phantom was developed by [7,8] as a biomimetic neural fiber phantom. This phantom consists of hollow coaxial electrospun (co-ES) microfibers made from Poly(ε-caprolactone) (PCL) and polyethylene oxide (PEO) comprising its shell and core components respectively. This material has already been shown to mimic brain white matter fibers using standard diffusion measurements (b-values up to 800 s/mm^2); however, in this paper we will examine the anomalous characteristics of these fibers using DTI at high b-values (up to 5000 s/mm^2).

This research is supported by the National Center for Advancing Translational Sciences (TL1TR000049) (AY), the National Institute of Biomedical Imaging and Bioengineering (NIH R01 EB007537) (RM), the project "CONNECT", the Future and Emerging Technologies (FET) Programme within the Seventh Framework Programme for Research of the European Commission, under FET-Open grant number: 238292 (FZ) and by a research grant from Philips Healthcare (PH).

Allen Ye*, Ziying Yin, and Richard Magin are at the University of Illinois at Chicago, Chicago, IL 60607 USA (**Corresponding Author:* phone: 312-996-4947; e-mail: allenye2@uic.edu).

Penny Hubbard, Feng-Lei Zhou, and Geoff Parker are at the CRUK-EPSRC Cancer Imaging Centre in Cambridge and Manchester, University of Manchester, Manchester M13 9PT, United Kingdom.

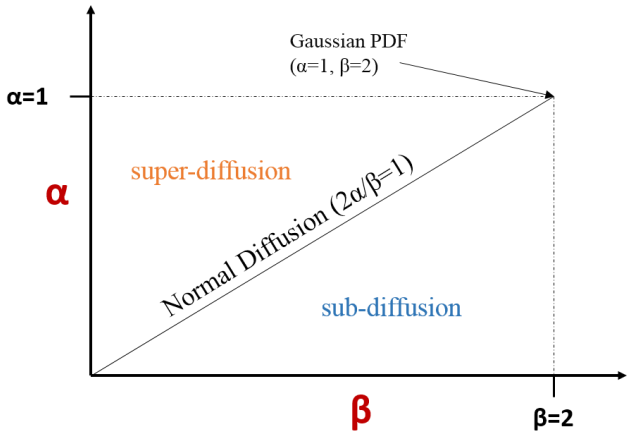

Figure 1. Continuous time random walk diffusion phase diagram with respect to α (time-fractional exponent) and β (space-fractional exponent).

II. Methods

A. Phantom Construction

A coaxial spinneret with two concentric needles was filled with a solution of PCL (outer needle) and PEO (inner needle). The outer needle was then connected to the positive terminal of a DC high voltage power supply and the fiber collector, placed some distance away from the concentric needles, was connected to the negative electrode. Two fiber orientations were produced, an aligned fiber phantom and a random fiber phantom. For the aligned fiber phantom, a voltage of 9 kV was applied and the PCL was pumped through the outer needle at 3 mL/hr while the inner solution flowed at 0.8 mL/hr. By limiting the inner core solution, fibers could have a controlled variable diameter. The collector was placed 5 cm away and careful control of the deposition process was maintained to align the fibers. The resultant fibers were then collected onto a wide drum, spinning at 800 rotations per minute, and allowed to dry. For the random fiber phantom, a voltage of 16.5 kV was applied with 3 mL/hr of PCL and 0.8 mL/hr of PEO pumped through the spinneret. In this case, the collector was placed 14 cm away and the drum was slowed to 150 rotations per minute, generating a uniform orientation distribution of fibers due to the break-down of uniform polymer flow at large distances. In both cases, the final evaporation of the inner core solution left hollow PCL fibers for DTI testing purposes.

B. Phantom Characterization

Microarchitecture of these fibers was visualized using a Phenom G2 desktop scanning electron microscope (SEM) with an accelerating voltage of 5 kV. The phantoms were frozen in liquid nitrogen then cut with a scalpel to expose the cross section, then coated with a thin layer of gold film in order to increase their electrical conductivity. Fibermetric software (Phenom, Eindhoven, Netherlands) was used to measure inner diameters of the fibers via its "Pore Measurement" function. For each sample, 10 different SEM images were selected and manually converted into the inner fiber diameters.

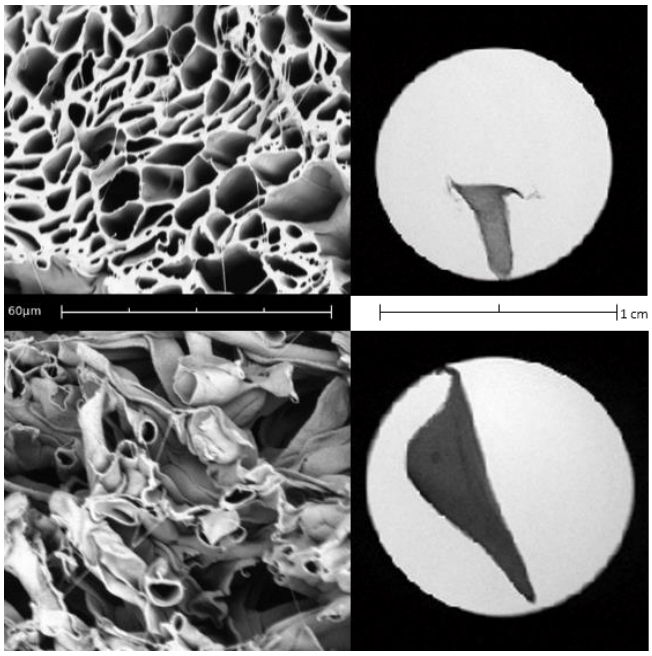

Figure 2. Aligned fibers (top) and random fibers (bottom) are shown alongside the MR image of the cross section of each fiber immersed in cyclohexane.

C. Diffusion Tensor Magnetic Resonance Imaging

Phantoms to be imaged were immersed in a 10 mm glass tube of cyclohexane (Sigma-Aldrich, St. Louis, MO, 99.5%) for 7 days to fully solvate the samples. Previous studies have shown that solvation in cyclohexane maintains fiber cohesion and does not promote swelling or shrinking of the fibers [7]. Cyclohexane has also been shown to enter the pores in the material, is MR-visible, and has a similar diffusion coefficient to water in biological tissues [9].

DTI was performed on a 9.4 T Agilent Small Animal Imaging system using a standard diffusion spin-echo pulse sequence with 6 directions and a b = 0 s/mm^2 image. MR images were acquired with a TR of 2000 ms, TE of 30 ms, FOV of 3 cm x 3 cm, matrix size of 256x256, slice thickness of 1 mm. Diffusion parameters included 6 b-values that ranged from 0-5000 s/mm^2, Δ = 20 ms, δ = 2 ms. The diffusion gradients included two directions that spanned in plane (across the fibers) and four directions that spanned perpendicular to the imaging plane (along the fibers) in pattern that sampled q-space evenly.

D. Magnetic Resonance Image Analysis

Custom software was written in Matlab (Mathworks, MA, USA) to analyze this data. A fully enclosed toolbox was created that accepts raw data from either Bruker or Agilent magnets and allows for region of interest (ROI) selections to calculate the diffusion parameters (both mono-exponential and CTRW). For each slice, ROIs were averaged and then fit to determine the apparent diffusion coefficient (ADC) and diffusion parameters. Tractography was also performed using TrackVis [10] and following the fiber assignment by continuous tracking (FACT) algorithm [11]. Tractography was masked using the b = 0 s/mm^2 and fractional anisotropy

(FA) images with an angle threshold of 60° and an FA threshold of 0.2.

III. Results

A. Fiber Structure

Micrographs from SEM had their area-weighted mean inner diameters measured as 10.2 ± 1.6 μm which mirrors large axons in white matter [12]. Fig. 2 shows an electron micrograph of the cross section of the aligned and random fibers along a cross section placed next to its corresponding MR image.

B. Mono-exponential Diffusion Parameters

Images taken at b = 0 s/mm^2 and 1500 s/mm^2 were considered when looking at mono-exponential diffusion parameters. ROIs were limited to central portions of the fibers in order to avoid any possible edge variation during the synthesis of these phantoms. We measured the FA, apparent diffusion coefficient (ADC), the mean diffusivity (MD), the axial diffusivity (AD), and radial diffusivity (RD) in the free cyclohexane surrounding the phantoms, as well as each of the two phantoms. Table 1 displays our results using the standard Gaussian diffusion model.

TABLE I. Mono-exponential Diffusion Parameters for Cyclohexane and two Fiber phantoms

	ADC (10^{-3} mm^2/s)	FA	MD (mm^2/s)	AD ∥ (mm^2/s)	RD ⊥ (mm^2/s)
C_6H_{12}	1.16	0.11	1.76E-03	1.94E-03	1.67E-03
Aligned	0.48	0.64	7.23E-04	1.34E-03	4.15E-04
Random	0.49	0.31	7.19E-04	9.42E-04	6.08E-04

C. Continuous Time Random Walk Diffusion Parameters

Instead of just looking at two b-values, CTRW requires an array of b-values to define the Mittag-Leffler function and derive the two fractional exponents (α, β) that govern the diffusion in these fibers. Because the CTRW model can only describe diffusion in a single dimension, we analyzed each of the six directions individually to derive the CTRW parameters for diffusion. To simplify analysis, we grouped each of these six directions into diffusion parallel with the main orientation of the fibers (4 of 6 directions) and diffusion perpendicular to the main orientation, across the fiber walls (2 of 6 directions). We found that for the free cyclohexane, as well as diffusion along the fibers, the 2α/β parameter gave values very close to 1, indicating standard diffusion. However, for directions that were perpendicular to the fibers, α was 0.63 for aligned fibers and 0.80 for random fibers, β was close to 2 leading to a 2α/β of less than 1, demonstrating sub-diffusion. Table 2 shows the complete array of values for both α and β and Fig. 3 shows the diffusion decay profiles for aligned and random fibers both along and against the primary orientation of the fibers.

TABLE II. Continuous Time Random Walk Parameters for Cyclohexane and two Fiber phantoms Against (⊥) and Along(∥) the fibers

	Align ⊥	Random ⊥	C_6H_{12} ⊥	Align ∥	Random ∥	C_6H_{12} ∥
α	0.63	0.80	0.99	0.99	0.96	0.97
β	1.99	2.00	2.00	1.98	2.00	1.99
2α/β	0.63	0.79	0.99	1.00	0.96	0.99

D. Fiber Tractography

Fiber tractography results matched the desired results of the collection process in creating both aligned and random fibers. Fiber estimation images can be seen in fig. 4 with the b=0 image shown in the background. In this color-coded image, blue represents z-axis orientation (∥ to fibers) while green and red represent x/y-axis orientation (⊥ to fibers).

IV. Discussion

The desire to establish the ground truth in diffusion tensor MRI has been approached by multiple methods. Software simulations [13], histological correlations [14], and physical phantoms [15] have all been used in order to better understand the results from DTI. Co-ES fibers have been proposed as a physical phantom that has basic geometry that matches very closely to those seen in white matter [16]. However, these co-ES fibers have only been investigated in the mono-exponential diffusion framework. It has been shown that white and gray matter in the brain exhibit

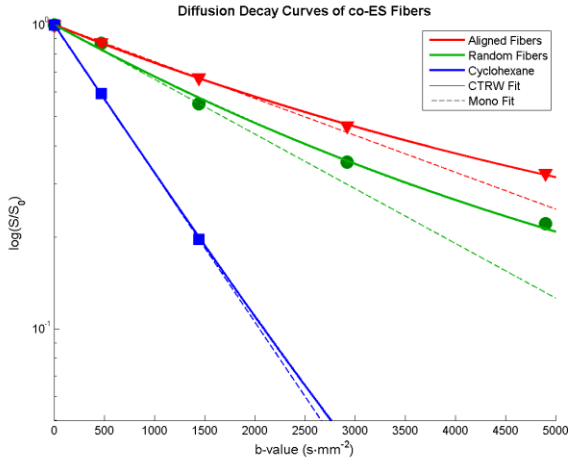

Figure 3. Diffusion decay curves for aligned fibers, random fibers, and free cyclohexane in the in-plane (⊥) direction. Fitting using CTRW uses a solid line while mono-exponential fitting uses dashed line. We can see that both aligned and random fibers deviate at high b-values (b>1500 mm/s^2) from the mono-exponential fit.

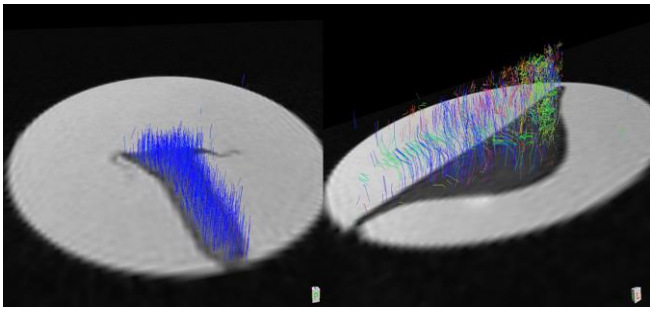

Figure 4. MR tractography showing the difference between the aligned fibers (left) and the random fibers (right). The background shows the b0-image for reference. As seen by the color-coding, the aligned fibers all exhibit z-axis orientation whereas the random fibers have less uniformity exhibiting both red and green colors (in-plane orientation) as well.

anomalous diffusion characteristics [4] and in this paper we planned to validate these co-ES fibers by broadening the assumptions made by molecular self-diffusion and examining these fibers using the CTRW model. Previous studies using the CTRW model have shown that the $2\alpha/\beta$ parameter ranges from 0.45 to 0.74 in the corpus callosum (white matter) and 0.68 to 0.84 in the cortex (gray matter) [6]. For our two samples, we had values of 0.63 for the aligned fibers and 0.80 for the random fibers leading us to believe that each of these fiber configurations could be valuable phantoms for mimicking brain architecture for white and gray matter respectively.

While the average inner fiber diameter is 10.2 μm, over 50% of the fibers have an inner diameter of less than 6 μm and some fibers are up to 40 μm in size [8]. Given such heterogeneous compartment sizes, it is perhaps not surprising that the standard mono-exponential modeling fails at high b values (as seen by signal deviation in Figure 3). An interesting thing to note from our results is that the β (space dependent fractional) parameter remained relatively constant whereas the α (time dependent fractional) parameter varied – at least in the perpendicular case, across the fibers. Using equation (1), we can estimate that water is able to travel approximately 6 μm during our diffusion experiment during the Δ (20 ms). By looking at our results, we can infer that jump-length is perhaps not as affected as much as waiting time between jumps. Instead of free diffusion, we can imagine molecules of cyclohexane trapped in the microstructure of the PCL shells, leading to sub-diffusion; this could potentially represent a process of permeation through the shell material. However, when we orient the diffusion gradients along these fibers, there are fewer diffusion hindering compartments, and we observe both a higher relative diffusion coefficient and a more normal (Gaussian) diffusion process.

By looking at the mono-exponential characteristics of the random fibers, we can see the axial diffusivity is 54% higher than the radial diffusivity. As compared to free cyclohexane which AD and RD only varied by 16%, we can infer that the random fibers may have a preferred fiber orientation that is mixed with fibers in other directions. This mirrors the actual structure of brain tissue as fibers often cross or kiss [17]. In the future, careful alignment during the synthesis of co-ES microfibers could lead to more controlled phantoms to mimic this architecture.

To our knowledge, this is the first attempt at using fractional parameters to characterize co-ES fibers. For the CTRW model, this paper demonstrates its utility in probing microarchitecture at a level that is not visible using standard diffusion sequences. For co-ES fibers, this shows their utility as a biomimetic DTI brain phantom, simulating both the mono-exponential and the anomalous characteristics of neural tissue. Future studies can include studying the difference between the CTRW model and other diffusion models such as those with multiple exponentials (CHARMED [18], IVIM [19]) or with different fractional exponents (e.g. stretched exponential [3]).

ACKNOWLEDGMENTS

A.Y. would like to thank Carson Ingo with his help in fitting the CTRW model and both Kaya Yasar and Mary Kim for their assistance in creating the tractography images.

REFERENCES

[1] H. Johansen-Berg and T. E. J. Behrens, *Diffusion MRI: From quantitative measurement to in-vivo neuroanatomy*. Academic Press, 2009.
[2] R. M. Mazo, *Brownian motion: fluctuations, dynamics, and applications*. Clarendon press Oxford, 2002.
[3] K. M. Bennett, K. M. Schmainda, R. Bennett (Tong), D. B. Rowe, H. Lu, and J. S. Hyde, "Characterization of continuously distributed cortical water diffusion rates with a stretched-exponential model," *Magn. Reson. Med.*, vol. 50, no. 4, pp. 727–734, Oct. 2003.
[4] X. J. Zhou, Q. Gao, O. Abdullah, and R. L. Magin, "Studies of anomalous diffusion in the human brain using fractional order calculus," *Magn. Reson. Med.*, vol. 63, no. 3, pp. 562–569, Mar. 2010.
[5] M. G. Hall and T. R. Barrick, "From diffusion-weighted MRI to anomalous diffusion imaging," *Magn. Reson. Med.*, vol. 59, no. 3, pp. 447–455, Mar. 2008.
[6] C. Ingo, R. L. Magin, L. Colon-Perez, W. Triplett, and T. H. Mareci, "On random walks and entropy in diffusion-weighted magnetic resonance imaging studies of neural tissue: Random Walks and Entropy in Diffusion-Weighted MRI," *Magn. Reson. Med.*, vol. 71, no. 2, pp. 617–627, Feb. 2014.
[7] F.-L. Zhou, P. L. Hubbard, S. J. Eichhorn, and G. J. M. Parker, "Coaxially Electrospun Axon-Mimicking Fibers for Diffusion Magnetic Resonance Imaging," *ACS Appl. Mater. Interfaces*, vol. 4, no. 11, pp. 6311–6316, Nov. 2012.
[8] P. L. Hubbard, F.-L. Zhou, S. J. Eichhorn, and G. J. M. Parker, "Biomimetic phantom for the validation of diffusion magnetic resonance imaging: Biomimetic Phantom for the Validation of dMRI," *Magn. Reson. Med.*, p. n/a–n/a, Jan. 2014. DOI: 10.1002/mrm.25107
[9] P. s. Tofts, D. Lloyd, C. a. Clark, G. j. Barker, G. j. m. Parker, P. McConville, C. Baldock, and J. m. Pope, "Test liquids for quantitative MRI measurements of self-diffusion coefficient in vivo," *Magn. Reson. Med.*, vol. 43, no. 3, pp. 368–374, 2000.
[10] R. Wang, T. Benner, A. G. Sorenson, and V. J. Wedeen, "Diffusion Toolkit: A Software Package for Diffusion Imaging Data Processing and Tractography," in *ISMRM Abstract*, 2007.
[11] S. Mori, B. J. Crain, V. P. Chacko, and P. C. M. Van Zijl, "Three-dimensional tracking of axonal projections in the brain by magnetic resonance imaging," *Ann. Neurol.*, vol. 45, no. 2, pp. 265–269, 1999.
[12] J. A. Perge, J. E. Niven, E. Mugnaini, V. Balasubramanian, and P. Sterling, "Why do axons differ in caliber?," *J. Neurosci.*, vol. 32, no. 2, pp. 626–638, 2012.
[13] T. G. Close, J.-D. Tournier, F. Calamante, L. A. Johnston, I. Mareels, and A. Connelly, "A software tool to generate simulated white matter structures for the assessment of fibre-tracking algorithms," *NeuroImage*, vol. 47, no. 4, pp. 1288–1300, 2009.
[14] J. J. Flint, B. Hansen, M. Fey, D. Schmidig, M. A. King, P. Vestergaard-Poulsen, and S. J. Blackband, "Cellular-level diffusion tensor microscopy and fiber tracking in mammalian nervous tissue with direct histological correlation," *Neuroimage*, vol. 52, no. 2, pp. 556–561, 2010.
[15] E. Farrher, J. Kaffanke, A. A. Celik, T. Stöcker, F. Grinberg, and N. J. Shah, "Novel multisection design of anisotropic diffusion phantoms," *Magn. Reson. Imaging*, vol. 30, no. 4, pp. 518–526, May 2012.
[16] P. Loui and G. Schlaug, "Investigating Musical Disorders with Diffusion Tensor Imaging: A Comparison of Imaging Parameters," *Ann. N. Y. Acad. Sci.*, vol. 1169, no. 1, pp. 121–125, Jul. 2009.
[17] D. S. Tuch, T. G. Reese, M. R. Wiegell, and V. J. Wedeen, "Diffusion MRI of complex neural architecture," *Neuron*, vol. 40, no. 5, pp. 885–895, 2003.
[18] Y. Assaf and P. J. Basser, "Composite hindered and restricted model of diffusion (CHARMED) MR imaging of the human brain," *Neuroimage*, vol. 27, no. 1, pp. 48–58, 2005.
[19] D. Le Bihan, E. Breton, and D. Lallemand, "Perfusion in intravoxel incoherent motion MR imaging," *Radiology*, vol. 168, pp. 497–505, 1988.